

# InterCLIP-MEP: Interactive CLIP and Memory-Enhanced Predictor for Multi-modal Sarcasm Detection

Junjie Chen<sup>1</sup>, Hang Yu<sup>2,\*</sup>, Weidong Liu<sup>3</sup>, Subin Huang<sup>1,†</sup>, Sanmin Liu<sup>1</sup>

<sup>1</sup> Key Laboratory of Computer Application Technology

School of Computer and Information, Anhui Polytechnic University, Anhui, China

<sup>2</sup> Shanghai University, Shanghai, China

<sup>3</sup> Inner Mongolia University, Inner Mongolia, China

gorji.chen@gmail.com, yuhang@shu.edu.cn, cslwd@imu.edu.cn, subinhuang@ahpu.edu.cn, sanmin.liu@ahpu.edu.cn

## Abstract

The prevalence of sarcasm in social media, conveyed through text-image combinations, presents significant challenges for sentiment analysis and intention mining. Existing multi-modal sarcasm detection methods have been proven to over-estimate performance, as they struggle to effectively capture the intricate sarcastic cues that arise from the interaction between an image and text. To address these issues, we propose InterCLIP-MEP, a novel framework for multi-modal sarcasm detection. Specifically, we introduce an Interactive CLIP (InterCLIP) as the backbone to extract text-image representations, enhancing them by embedding cross-modality information directly within each encoder, thereby improving the representations to capture text-image interactions better. Furthermore, an efficient training strategy is designed to adapt InterCLIP for our proposed Memory-Enhanced Predictor (MEP). MEP uses a dynamic, fixed-length dual-channel memory to store historical knowledge of valuable test samples during inference. It then leverages this memory as a non-parametric classifier to derive the final prediction, offering a more robust recognition of multi-modal sarcasm. Experiments demonstrate that InterCLIP-MEP achieves state-of-the-art performance on the MMSD2.0 benchmark, with an accuracy improvement of 1.08% and an F1 score improvement of 1.51% over the previous best method.

## Introduction

Sarcasm, with its inherent subtlety and complexity, plays a significant role in human communication by often conveying irony, mockery, or hidden intentions (Muecke 1982; Gibbs and O’Brien 1991; Gibbs and Colston 2007). The automatic detection of sarcasm from text has been a significant research focus, aiding tasks such as sentiment analysis and intent mining (Pang, Lee et al. 2008; Tsur, Davidov, and Rappoport 2010; Bouazizi and Ohtsuki 2015). With the rapid development of social media platforms like Twitter and Reddit, users frequently use text-image combinations to convey their messages. Therefore, the need for multi-modal sarcasm detection has become increasingly apparent, which presents significant challenges, requiring the system to capture and comprehend the intricate interplay between textual and visual information to identify sarcasm cues.

\*Co-corresponding. Email: yuhang@shu.edu.cn

†Corresponding author. Email: subinhuang@ahpu.edu.cn

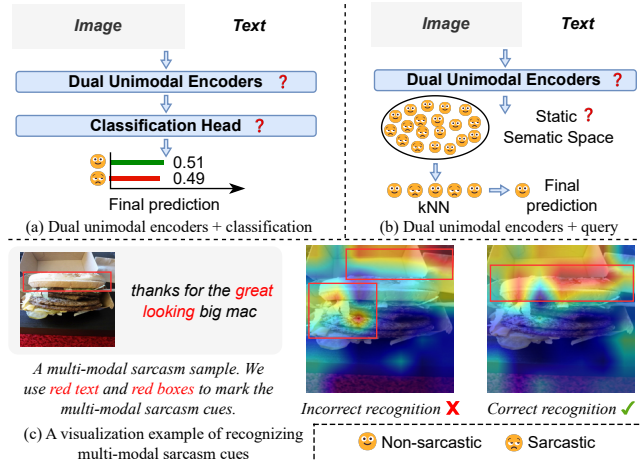


Figure 1: An overview of the shortcomings of existing multi-modal sarcasm detection pipelines. In panels (a) and (b), we present two multi-modal sarcasm detection pipelines, with shortcomings indicated by a red question mark. In panel (c), we visually show an example of multi-modal sarcasm cues correctly or incorrectly recognized in a sarcasm sample.

Despite the notable advancements made by existing studies (Xu, Zeng, and Mao 2020; Pan et al. 2020; Liang et al. 2021, 2022) in this field, Qin et al. (2023) have highlighted that the MMSD benchmark (Cai, Cai, and Wan 2019) employed in these works contains spurious cues. These cues lead to the development of biased models, thereby inflating the perceived effectiveness of these models in detecting sarcasm cues from multi-modal data. By introducing MMSD2.0, a refined benchmark that eliminates spurious cues and corrects mislabeled samples, Qin et al. (2023) demonstrates a substantial performance decline of existing methods when evaluated on MMSD2.0. Although they proposed a promising method that employs a Multi-view CLIP for reliable multi-modal sarcasm detection, it still leaves room for improvement, similar to their previous approaches.

As shown in Figure 1(a) and Figure 1(b), some existing methods (Xu, Zeng, and Mao 2020; Pan et al. 2020; Liang et al. 2021, 2022; Wen, Jia, and Yang 2023; Tian et al. 2023; Wei et al. 2024) use dual unimodal encoders,

such as BERT (Devlin et al. 2019) for text and ViT (Dosovitskiy et al. 2021) for image, as the backbone to encode samples. This approach makes it difficult for the model to capture the subtle interactive information between text and image. Although Qin et al. (2023) utilized a multi-modal pre-trained backbone, CLIP (Radford et al. 2021), to encode samples and demonstrated notable results on the MMSD2.0 benchmark, the original CLIP only aligns text and images directly, lacking the nuanced semantic space required for sarcasm detection. To illustrate the identification of multi-modal sarcasm cues, we present in Figure 1(c) an example of a sarcasm sample being correctly and incorrectly recognized. Furthermore, as depicted in Figure 1(a), some approaches (Xu, Zeng, and Mao 2020; Pan et al. 2020; Liang et al. 2021, 2022; Wen, Jia, and Yang 2023; Tian et al. 2023) directly classify sarcastic samples based on their representations. This often leads to high prediction entropy and erroneous outcomes, especially for hard cases with greater uncertainty. To the best of our knowledge, only Wei et al. (2024) considers leveraging historical knowledge of samples to aid in detection. As shown in Figure 1(b), they constructed a static semantic space that stores features of all training samples. When identifying sarcastic samples, they query  $k$ -nearest neighbors in this semantic space and use a voting mechanism to derive the final predictions. However, relying heavily on a static semantic space may limit its ability to adapt to various test samples.

In this paper, building on these insights, we propose InterCLIP-MEP, a novel framework designed to enhance the reliability of multi-modal sarcasm detection. Our InterCLIP-MEP introduces a refined variant of CLIP, Interactive CLIP (InterCLIP), as the backbone to enhance sample encoding for detecting multi-modal sarcasm. InterCLIP enhances the capture of interactive information between text and image by embedding representations from one modality into the encoder of the other, leading to a more nuanced understanding of multi-modal sarcasm cues. During inference, Our InterCLIP-MEP introduces a Memory-Enhanced Predictor (MEP) to build dynamically a non-parametric classifier from valuable historical features to identify multi-modal sarcasm. Specifically, we design an efficient training strategy to adapt InterCLIP for MEP. Based on the sample representations encoded by InterCLIP, we train a classification module to assign pseudo-labels to samples. Simultaneously, we train a projection module to map samples into a latent space. In this latent space, same-class samples are pulled closer together, while different-class samples are pushed further apart. Additionally, we fine-tune the weights of the self-attention modules in InterCLIP’s text and vision encoders using the low-rank adaptation (LoRA) technique (Hu et al. 2022), building upon the original CLIP weights. This approach allows for more efficient adaptation without significantly increasing the computational burden. Building on InterCLIP and the training strategy, MEP leverages historical knowledge of valuable test samples to identify multi-modal sarcasm. It maintains a dynamic, fixed-length dual-channel memory, with one channel storing historical information of non-sarcastic samples and the other storing information of sarcastic samples. MEP then utilizes this memory as a non-

parametric classifier to compute the final prediction for each sample, offering more robust and reliable multi-modal sarcasm detection.

Overall, our contributions can be summarized as follows:

- We propose InterCLIP-MEP, a novel framework for reliable multi-modal sarcasm detection, which introduces Interactive CLIP (InterCLIP) improving the encoding of text-image interactions by embedding cross-modality information within each encoder and Memory-Enhanced Predictor (MEP) offering more robust and reliable multi-modal sarcasm detection.
- We develop an efficient training strategy that ensures computational efficiency and superior performance, bridging InterCLIP and MEP.
- Our extensive experiments on the more reliable benchmark, MMSD2.0, demonstrate that InterCLIP-MEP<sup>1</sup> outperforms existing state-of-the-art methods.

## Related Work

**Multi-modal sarcasm detection.** Early work in sarcasm detection primarily focused on textual data (Bouazizi and Ohtsuki 2015; Amir et al. 2016; Baziotis et al. 2018). With the rise of social media, detecting sarcasm from text-image data has become increasingly challenging, leading to the development of several multi-modal approaches. Schifanella et al. (2016) were among the first to use multi-modal posts from social platforms to identify sarcasm cues from both text and images. Cai, Cai, and Wan (2019) introduced the MMSD benchmark for multi-modal sarcasm detection, demonstrating its effectiveness with a hierarchical fusion model incorporating image attributes. This benchmark has been widely used in subsequent studies (Xu, Zeng, and Mao 2020; Pan et al. 2020; Liang et al. 2021, 2022; Liu, Wang, and Li 2022; Qin et al. 2023; Wen, Jia, and Yang 2023; Tian et al. 2023; Wei et al. 2024). However, MMSD has been proven to contain spurious cues that could bias models (Qin et al. 2023). To address this, Qin et al. (2023) introduced the MMSD2.0 benchmark, which removed these cues and corrected mislabeled samples. They observed a significant performance drop when re-evaluating state-of-the-art methods on MMSD2.0 and proposed the need for more stable multi-modal sarcasm detection methods. In this work, we introduce the InterCLIP-MEP framework towards more reliable multi-modal sarcasm detection.

**CLIP adaptation.** The Contrastive Language-Image Pretraining (CLIP) model (Radford et al. 2021) excels in vision-language tasks. Adapting CLIP for specific domains has shown substantial improvements, as demonstrated by Li, Shakhnarovich, and Yeh (2022) for phrase localization, Liang et al. (2023) for open-vocabulary semantic segmentation, and Wang et al. (2023) for action recognition. In this work, inspired by Ganz et al. (2024), we conditionally enhance both the text and visual encoders of CLIP, making it more effective in capturing the interplay between text and images to identify sarcasm. Unlike Ganz et al. (2024), who focused solely on embedding text into the visual encoder, we

<sup>1</sup><https://github.com/CoderChen01/InterCLIP-MEP>

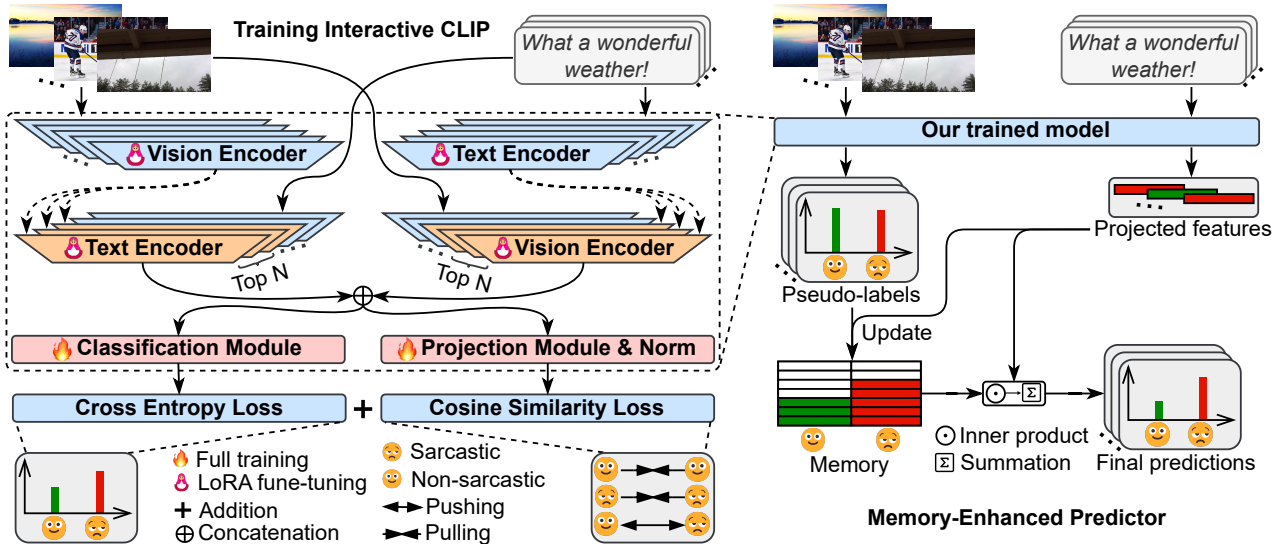


Figure 2: Overview of our framework. **Training Interactive CLIP (InterCLIP)**. Vision and text representations are extracted using separate encoders and embedded into the top- $n$  layers of the opposite modality’s encoder for interaction. The top- $n$  layers are fine-tuned with LoRA, while the rest of the encoder remains frozen. Final vision and text representations are concatenated and used to train a classification module for sarcasm detection. A projection module is also trained to project representations into a latent space. **Memory-Enhanced Predictor (MEP)**. During inference, InterCLIP generates interactive representations. The classification module assigns pseudo-labels, and the projection module provides projection features. MEP updates dynamic memory with these features and pseudo-labels. The final prediction is made by comparing the current sample’s projected feature with those in memory.

also explore embedding images into the text encoder. Furthermore, their approach is limited to general classification tasks and does not address the complexities of multi-modal sarcasm detection.

**Memory-enhanced prediction.** Inspired by cognitive science (Stokes 2015; Baddeley 2000), memory has been introduced to enhance neural networks (Weston, Chopra, and Bordes 2014; Sukhbaatar et al. 2015). Several studies (Wu et al. 2018; Wen, Jia, and Yang 2023) have used memory mechanisms to improve model training, and some (Zhang et al. 2024; Wei et al. 2024) leverage memory to store historical knowledge, enhancing prediction accuracy. In this work, we introduce a memory-enhanced predictor for multi-modal sarcasm detection. In contrast to other methods, our memory dynamically updates during testing, utilizing relevant historical information for improved accuracy and robustness.

## Methodology

An overview of InterCLIP-MEP is illustrated in Figure 2. Initially, we elaborate on the Interactive CLIP (InterCLIP) and its training strategy, followed by an in-depth explanation of the Memory-Enhanced Predictor (MEP).

### Interactive CLIP

The input to Interactive CLIP (InterCLIP) is a text-image pair  $\mathcal{P} = (T, I)$ , where  $T$  represents a piece of text and  $I$  represents an image. Here, for simplicity, we do not consider the case of batch inputs. The text encoder  $\mathcal{T}$  extracts the

vanilla text representation  $\mathbf{F}_t$ :

$$\mathbf{F}_t = \mathcal{T}(T) = \{h_{\text{bos}}^t(t_{\text{bos}}), h_1^t(t_1), \dots, h_n^t(t_n), h_{\text{eos}}^t(t_{\text{eos}})\}, \quad (1)$$

where  $t_i$  denotes a text token,  $n$  is the length of  $T$  after tokenization,  $t_{\text{bos}}$  and  $t_{\text{eos}}$  are special tokens required by the text encoder. Here,  $h_i^t(\cdot) \in \mathbb{R}^{d_t}$  represents the  $d_t$ -dimensional encoded representation of the corresponding token  $t_i$ , with  $i$  ranging from 1 to  $n$ , including the beginning-of-sequence (bos) and end-of-sequence (eos) tokens. The vision encoder  $\mathcal{V}$  extracts the vanilla image representation  $\mathbf{F}_v$ :

$$\mathbf{F}_v = \mathcal{V}(I) = \{h_{\text{cls}}^v(p_{\text{cls}}), h_1^v(p_1), \dots, h_m^v(p_m)\}, \quad (2)$$

where  $I$  is processed into multiple patches  $p_i$ ,  $m$  is the number of patches, and  $p_{\text{cls}}$  is a special token required by the visual encoder. Here,  $h_i^v(\cdot) \in \mathbb{R}^{d_v}$  represents the  $d_v$ -dimensional encoded representation of the corresponding  $p_i$ , with  $i$  ranging from 1 to  $m$ , including the classification (cls) token. Specifically, both  $\mathbf{F}_t$  and  $\mathbf{F}_v$  are representations from the final layer outputs of their respective encoders. Conditioning on  $\mathbf{F}_t$  or  $\mathbf{F}_v$ , we can obtain the interactive text representation  $\tilde{\mathbf{F}}_t$  or the interactive image representation  $\tilde{\mathbf{F}}_v$ :

$$\tilde{\mathbf{F}}_t = \mathcal{T}(T|\mathbf{F}_v), \tilde{\mathbf{F}}_v = \mathcal{V}(I|\mathbf{F}_t). \quad (3)$$

We use  $\tilde{h}_i^t(\cdot) \in \mathbb{R}^{d_t}$  and  $\tilde{h}_i^v(\cdot) \in \mathbb{R}^{d_v}$  to denote the re-encoded interactive representations of each text token and image patch, respectively.

To be specific, we condition only the top- $n$  self-attention layers of the text or vision encoder, where  $n$  is a hyperparameter that will be analyzed in the experiment section. Figure 3

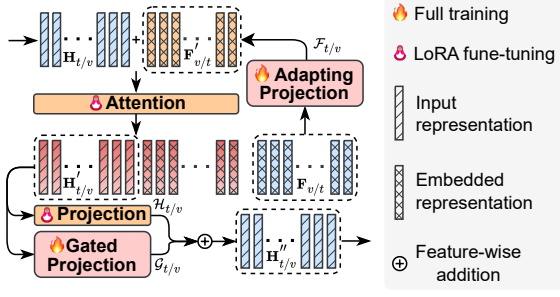


Figure 3: Structure of the conditional self-attention layer.

illustrates the structure of the conditioned self-attention layers. Given that the text and vision encoder in CLIP share a similar architecture, for simplicity, we denote the input representations to the self-attention layers of the text or vision encoder as  $\mathbf{H}_{t/v}$ , which are derived from the outputs of the previous layer. The previous layer can either be conditioned or non-conditioned. Due to the dimensional mismatch between the embedded representations  $\mathbf{F}_{v/t}$  and the corresponding encoder representation space, we introduce an adapting projection layer  $\mathcal{F}_{t/v}$  to project  $\mathbf{F}_{v/t}$  into the appropriate representation space.

To fuse the input representations  $\mathbf{H}_{t/v}$  with the projected embedded representations  $\mathbf{F}'_{v/t} = \mathcal{F}_{t/v}(\mathbf{F}_{v/t})$ , we concatenate them and feed them into the attention layer to obtain the transformed representations. We then extract the transformed input representations  $\mathbf{H}'_{t/v}$  from the output. Following Ganz et al. (2024), we apply a gated projection layer  $\mathcal{G}_{t/v}$  along with the self-attention’s projection head  $\mathcal{H}_{t/v}$  using a learnable gating mechanism to compute the self-attention output representation  $\mathbf{H}''_{t/v}$ .

Given the similarity between the self-attention layers of the vision encoder and the text encoder, we use the text encoder  $\mathcal{T}$  to illustrate the process as follows:

$$\begin{aligned}
 \mathbf{F}'_v &= \mathcal{F}_t(\mathbf{F}_v), \quad \mathbf{F}_v \in \mathbb{R}^{m \times d_v}, \quad \mathbf{F}'_v \in \mathbb{R}^{m \times d_t}, \\
 \mathbf{H}'_t &= \text{Attn}_t(\mathbf{H}_t \oplus \mathbf{F}'_v)_{[n]}, \\
 \mathbf{H}_t, \mathbf{H}'_t &\in \mathbb{R}^{n \times d_t}, \quad \mathbf{H}_t \oplus \mathbf{F}'_v \in \mathbb{R}^{(n+m) \times d_t}, \\
 \mathbf{H}''_t &= \mathcal{H}_t(\mathbf{H}'_t) + \mathcal{G}_t(\mathbf{H}'_t) \cdot \tanh(\beta_t), \quad \mathbf{H}''_t \in \mathbb{R}^{n \times d_t}.
 \end{aligned} \tag{4}$$

Here,  $\oplus$  denotes the concatenation operation, and  $\beta_t$  is a learnable parameter initialized to 0 to ensure training stability. The subsequent computation follows the original CLIP (Radford et al. 2021), ultimately yielding the interactive representations  $\tilde{\mathbf{F}}_t$ .

InterCLIP has three distinct modes to achieve the final fused feature  $\tilde{h}^f \in \mathbb{R}^{d_t+d_v}$ :

- **T2V**: The text encoder extracts the vanilla text representation  $\mathbf{F}_t$ . This text representation is then embedded into the vision encoder to obtain the conditioned vision representation  $\tilde{\mathbf{F}}_v$ . The final fused representation  $\tilde{h}^f$  is formed by concatenating  $h^t_{\text{eos}}(t_{\text{eos}})$  and  $\tilde{h}^v_{\text{cls}}(p_{\text{cls}})$ .
- **V2T**: The vision encoder extracts the vanilla image representation  $\mathbf{F}_v$ . This image representation is then embed-

ded into the text encoder to obtain the conditioned text representation  $\tilde{\mathbf{F}}_t$ . The final fused representation  $\tilde{h}^f$  is formed by concatenating  $\tilde{h}^t_{\text{eos}}(t_{\text{eos}})$  and  $h^v_{\text{cls}}(p_{\text{cls}})$ .

- **Two-way (TW)**: The text and vision encoders extract the vanilla text and image representations  $\mathbf{F}_t$  and  $\mathbf{F}_v$ , respectively. These representations are then embedded into the vision and text encoders to obtain the conditioned image representation  $\tilde{\mathbf{F}}_v$  and text representation  $\tilde{\mathbf{F}}_t$ . The final fused representation  $\tilde{h}^f$  is formed by concatenating  $\tilde{h}^t_{\text{eos}}(t_{\text{eos}})$  and  $\tilde{h}^v_{\text{cls}}(p_{\text{cls}})$ .

We will analyze the effectiveness of these three modes of interaction in the experimental analysis.

## Training Strategy

As shown in Figure 2 (left), to adapt InterCLIP for MEP, we introduce an efficient training strategy. Using InterCLIP as the backbone to obtain fused features of the samples, we introduce a classification module and a projection module.

The classification module  $\mathcal{F}_c$  calculates the probability of a sample being sarcastic or non-sarcastic:

$$\hat{y} = \text{softmax}(\mathcal{F}_c(\tilde{H}^f)), \tag{5}$$

where  $\tilde{H}^f \in \mathbb{R}^{N \times (d_t+d_v)}$  represents the fused representations of a batch of samples, and  $N$  denotes the batch size. We optimize  $\mathcal{F}_c$  using binary cross-entropy loss:

$$\mathcal{L}^c = -\frac{1}{N} \sum_{i=1}^N [y_i \log(\hat{y}_{i,1}) + (1 - y_i) \log(1 - \hat{y}_{i,1})], \tag{6}$$

where  $y_i$  denotes the label of the  $i$ -th sample, with sarcastic labeled as 1 and non-sarcastic as 0, and  $\hat{y}_i$  denotes the prediction for the  $i$ -th sample.

The projection module  $\mathcal{F}_p$  maps  $\tilde{H}^f$  into a latent feature space:

$$\hat{H}^f = \text{norm}(\mathcal{F}_p(\tilde{H}^f)), \quad \hat{H}^f \in \mathbb{R}^{N \times d_f}, \tag{7}$$

where  $\text{norm}(\cdot)$  denotes L2 normalization, and  $d_f$  represents the dimension of the projected features. In this space, the cosine distance between features of the same class is minimized, while the distance between features of different classes is maximized. We use a label-aware cosine similarity loss to optimize  $\mathcal{F}_p$ :

$$\begin{aligned}
 \mathcal{L}^p &= \text{mean}(\hat{H}_P^f \cdot \hat{H}_N^{fT}) + \text{mean}(1 - \hat{H}_P^f \cdot \hat{H}_P^{fT}) \\
 &\quad + \text{mean}(1 - \hat{H}_N^f \cdot \hat{H}_N^{fT}), \tag{8}
 \end{aligned}$$

where  $\hat{H}_P^f$  and  $\hat{H}_N^f$  represent the projected fused features of positive and negative samples, respectively.

We fully train the modules  $\mathcal{F}_c$ ,  $\mathcal{F}_p$ , the adapting projection layer  $\mathcal{F}_{t/v}$ , the gated projection layer  $\mathcal{G}_{t/v}$ , and the parameters  $\beta_{t/v}$ . We use LoRA (Hu et al. 2022) to fine-tune parts of the weight matrices  $\mathbf{W}$  in the self-attention modules of all encoders, specifically various combinations of  $W_q$ ,  $W_k$ ,  $W_v$ , and  $W_o$ . We consider  $\mathbf{W}$  and the rank  $r$  of LoRA as hyperparameters for our study. All modules are optimized by minimizing the joint loss:

$$\mathcal{L} = \mathcal{L}^c + \mathcal{L}^p. \tag{9}$$

---

**Algorithm 1: Memory-Enhanced Predictor**

---

**Input:** Memory size  $L$ , Learned InterCLIP model, classification module  $\mathcal{F}_c$  and projection module  $\mathcal{F}_p$

**Output:** Final prediction  $\hat{y}^p$

```
1: Initialize memory  $\mathcal{M} \in \mathbf{0}^{2 \times L \times d_f}$ 
2: Initialize index  $\mathcal{I} \in \mathbf{0}^2$ 
3: Initialize entropy records  $\mathcal{C} \in \mathbf{0}^{2 \times L}$ 
4: for  $i \leftarrow 1$  to  $N_{\text{test}}$  do
5:    $\tilde{h}_i^f \leftarrow \text{InterCLIP}(\mathcal{P}_i)$ 
6:    $\hat{y}_i \leftarrow \text{softmax}(\mathcal{F}_c(\tilde{h}_i^f))$ 
7:    $\ell_{\text{pse}_i} \leftarrow \arg \max_j (\hat{y}_{i,j}), j \in \{0, 1\}$ 
8:    $c_i \leftarrow -\hat{y}_{i,0} \log \hat{y}_{i,0} - \hat{y}_{i,1} \log \hat{y}_{i,1}$ 
9:    $\hat{h}_i^f \leftarrow \text{norm}(\mathcal{F}_p(\tilde{h}_i^f))$ 
10:  if  $\mathcal{I}[\ell_{\text{pse}_i}] < L$  then
11:     $\mathcal{M}[\ell_{\text{pse}_i}][\mathcal{I}[\ell_{\text{pse}_i}]] \leftarrow \hat{h}_i^f$ 
12:     $\mathcal{C}[\ell_{\text{pse}_i}][\mathcal{I}[\ell_{\text{pse}_i}]] \leftarrow c_i$ 
13:     $\mathcal{I}[\ell_{\text{pse}_i}] \leftarrow \mathcal{I}[\ell_{\text{pse}_i}] + 1$ 
14:  else
15:     $j \leftarrow \text{GetMaxIdx}(\mathcal{C}[\ell_{\text{pse}_i}])$ 
16:    if  $c_i < \mathcal{C}[\ell_{\text{pse}_i}][j]$  then
17:       $\mathcal{M}[\ell_{\text{pse}_i}][j] \leftarrow \hat{h}_i^f$ 
18:       $\mathcal{C}[\ell_{\text{pse}_i}][j] \leftarrow c_i$ 
19:    end if
20:  end if
21:   $\text{logits} \leftarrow [\sum_{k=0}^{\mathcal{I}[0]} (\hat{h}_i^f \mathcal{M}[0]^T)_k, \sum_{k=0}^{\mathcal{I}[1]} (\hat{h}_i^f \mathcal{M}[1]^T)_k]$ 
22:   $\hat{y}_i^p \leftarrow \text{softmax}(\text{logits})$ 
23:  yield  $\hat{y}_i^p$ 
24: end for
```

---

## Memory-Enhanced Predictor

As depicted in Figure 2 (right), we present the Memory-Enhanced Predictor (MEP) that builds upon the learned InterCLIP, along with the classification module and the projection module, leveraging the valuable historical knowledge of test samples to enhance sarcasm detection.

The detailed computational process of MEP is provided in Algorithm 1, where  $N_{\text{test}}$  denotes the number of test samples. MEP uses the trained InterCLIP to extract fused features of the samples. It utilizes the classification module  $\mathcal{F}_c$  to assign a pseudo-label  $\ell_{\text{pse}_i}$  to each sample  $\mathcal{P}_i$  and the projection module  $\mathcal{F}_p$  to obtain the sample’s projected feature  $\hat{h}_i^f$ . To store valuable projected features of test samples as historical knowledge, MEP maintains a dynamic fixed-length dual-channel memory  $\mathcal{M} \in \mathcal{R}^{2 \times L \times d_f}$ , where  $L$  is the memory length per channel. The first channel stores projected features of non-sarcastic samples, while the second channel stores those of sarcastic samples. Based on the pseudo-label  $\ell_{\text{pse}_i}$ , the appropriate memory channel  $\mathcal{M}[\ell_{\text{pse}_i}]$  is selected for updating. If the selected channel has available space, the sample’s projected features are added directly, and the prediction entropy is recorded. If the memory is full, the prediction entropy of all samples in the memory is compared with that of the current sample, replacing the samples with the highest entropy as necessary. Finally, the current sample’s projected features are combined with the historical features

---

	All	Sarcastic	Non-sarcastic
Train	19,812	9,572	10,240
Validation	2,410	1,042	1,368
Test	2,409	1,037	1,372

---

Table 1: Statistics of the dataset from the MMSD2.0 benchmark (Qin et al. 2023).

stored in both memory channels  $\mathcal{M}$  using cosine similarity to yield the final prediction.

## Experiment

### Experimental Settings

**Datasets.** We use the dataset from the MMSD2.0 benchmark (Qin et al. 2023), which is an improved version of the dataset originally introduced by Cai, Cai, and Wan (2019). We present the statistics of the dataset in Table 1.

**Metrics.** Following Liu, Wang, and Li (2022), we use accuracy (Acc.), precision (P), recall (R), and F1-score (F1) as metrics to evaluate the performance of our model.

**Baselines.** We compare the effectiveness of the InterCLIP-MEP framework against several unimodal and multi-modal methods. For text modality methods, we compare with TextCNN (Kim 2014), Bi-LSTM (Graves and Schmidhuber 2005), SMSD (Xiong et al. 2019), and RoBERTa (Liu et al. 2019). For image modality methods, we compare with ResNet (He et al. 2016) and ViT (Dosovitskiy et al. 2021). For state-of-the-art multi-modal methods, we compare with the following:

- HFM (Cai, Cai, and Wan 2019): A hierarchical fusion model integrating text and image features.
- Att-BERT (Pan et al. 2020): A model using an attention mechanism to capture sarcasm incongruity.
- CMGCN (Liang et al. 2022): A method that constructs a cross-modal graph and employs a graph convolutional network.
- HKE (Liu, Wang, and Li 2022): A hierarchical framework utilizing multi-head cross-attention and graph neural networks.
- DIP (Wen, Jia, and Yang 2023): A dual incongruity perceiving network that extracts sarcastic information from factual and affective levels.
- DynRT (Tian et al. 2023): A dynamic routing transformer network for multi-modal sarcasm detection.
- Multi-view CLIP (Qin et al. 2023): A method adapted to CLIP for capturing multi-view sarcasm cues.
- G<sup>2</sup>SAM (Wei et al. 2024): A method using global graph-based semantic awareness and leveraging historical knowledge from training samples for multi-modal sarcasm detection.

### Main Results

To validate the effectiveness of our InterCLIP-MEP framework, we conduct experiments using the original CLIP as

Modality	Method	Acc. (%)	F1 (%)	P (%)	R (%)
Text	TextCNN* (Kim 2014)	71.61	69.52	64.62	75.22
	Bi-LSTM* (Graves and Schmidhuber 2005)	72.48	68.05	68.02	68.08
	SMSD* (Xiong et al. 2019)	73.56	69.97	68.45	71.55
	RoBERTa* (Liu et al. 2019)	79.66	76.21	76.74	75.70
Image	ResNet* (He et al. 2016)	65.50	57.58	61.17	54.39
	ViT* (Dosovitskiy et al. 2021)	72.02	69.72	65.26	74.83
Text-Image	HFM* (Cai, Cai, and Wan 2019)	70.57	66.88	64.84	69.05
	Att-BERT* (Pan et al. 2020)	80.03	77.04	76.28	77.82
	CMGCN* (Liang et al. 2022)	79.83	76.90	75.82	78.01
	HKE* (Liu, Wang, and Li 2022)	76.50	72.25	73.48	71.07
	DIP <sup>†</sup> (Wen, Jia, and Yang 2023)	80.59	78.23	75.52	81.14
	DynRT <sup>†</sup> (Tian et al. 2023)	70.37	68.55	63.02	75.15
	Multi-view CLIP* (Qin et al. 2023)	<u>85.64</u>	<u>84.10</u>	<u>80.33</u>	<u>88.24</u>
	G <sup>2</sup> SAM <sup>†</sup> (Wei et al. 2024)	<u>79.43</u>	<u>78.07</u>	72.04	85.20
	InterCLIP-MEP w/o Inter ( $L = 1024$ )	<b>86.05</b>	<b>84.81</b>	79.83	<b>90.45</b>
	InterCLIP-MEP w/ TW ( $L = 128$ )	85.51	<b>84.26</b>	79.15	<b>90.07</b>
InterCLIP-MEP w/ V2T ( $L = 640$ )	<b>86.26</b>	<b>85.00</b>	80.17	<b>90.45</b>	
InterCLIP-MEP w/ T2V ( $L = 1024$ )	<b>86.72</b>	<b>85.61</b>	80.20	<b>91.80</b>	

Table 2: Main results. We use \* to indicate that the results are taken from Qin et al. (2023). † indicates the results obtained by running this method on the MMSD2.0 benchmark (Qin et al. 2023). Underlined values represent the best baseline for comparison. Bold values indicate those that surpass the baseline.

Variant	w/o Inter		w/ TW		w/ V2T		w/ T2V	
	Acc. (%)	F1 (%)	Acc. (%)	F1 (%)	Acc. (%)	F1 (%)	Acc. (%)	F1 (%)
BASELINE	<b>86.05</b>	<b>84.81</b>	<b>85.51</b>	<b>84.26</b>	<b>86.26</b>	<b>85.00</b>	<b>86.72</b>	<b>85.61</b>
w/o Proj	85.76	84.43	85.43	84.05	85.68	84.22	86.22	84.51
w/o MEP	85.39	83.99	85.22	83.79	86.26	84.78	86.26	84.82
w/o LoRA	82.44	77.73	76.42	74.37	73.31	72.22	75.13	71.79

Table 3: Ablation study of InterCLIP-MEP. BASELINE represents the results of the corresponding method without any ablation.

the backbone instead of InterCLIP, referred to as InterCLIP-MEP w/o Inter. We compare this configuration with three interaction modes of InterCLIP: InterCLIP-MEP w/ V2T, InterCLIP-MEP w/ T2V, and InterCLIP-MEP w/ TW.

For each experiment, we condition only the top four layers of the self-attention modules, with the projection dimension  $d_f$  set to 1024. We set the rank  $r$  of LoRA to 8, fine-tuning the self-attention module weight matrices  $\mathbf{W}$ , specifically  $W_k$ ,  $W_v$ , and  $W_o$ . For the memory size  $L$  of the MEP, we select the optimal size from  $\mathbf{L} = \{128, 256, 384, 512, 640, 768, 896, 1024, 1152, 1280\}$ .

The main results are shown in Table 2. Our framework consistently outperforms or matches the performance of state-of-the-art methods, whether using InterCLIP or the original CLIP as the backbone, as shown in Table 2. This demonstrates the effectiveness of our training strategy and MEP. Methods InterCLIP-MEP w/ V2T and InterCLIP-MEP w/ T2V outperform InterCLIP-MEP w/o Inter, indicating that InterCLIP more effectively captures text-image interactions. Additionally, InterCLIP-MEP w/ T2V outperforms InterCLIP-MEP w/ V2T, likely due to the complexity of the visual space, which poses challenges for the projection layer in mapping visual representations into the text

encoder space effectively. We observe that InterCLIP-MEP w/ TW performs worse than InterCLIP-MEP w/o Inter, possibly because embedding representations within both encoders increases learning difficulty compared to unidirectional methods. In summary, InterCLIP with T2V interaction, combined with our training strategy and MEP yields the most promising results.

### Ablation Study

To further validate the effectiveness of InterCLIP-MEP, we remove the projection module  $\mathcal{F}_p$  and train only the classification module  $\mathcal{F}_c$  for prediction, denoted as w/o Proj. To test the necessity of using LoRA (Hu et al. 2022) for fine-tuning, we keep the rest of InterCLIP-MEP unchanged and freeze all self-attention weight matrices of InterCLIP, denoted as w/o LoRA, always selecting the optimal memory size  $L$  for the MEP during inference. To evaluate the effectiveness of the MEP, we train both  $\mathcal{F}_p$  and  $\mathcal{F}_c$  but use only  $\mathcal{F}_c$  during inference, denoted as w/o MEP.

Table 3 reports all results. All variants show performance declines compared to the baseline, demonstrating the importance of each module in the InterCLIP-MEP framework. For methods InterCLIP-MEP w/ TW and InterCLIP-MEP



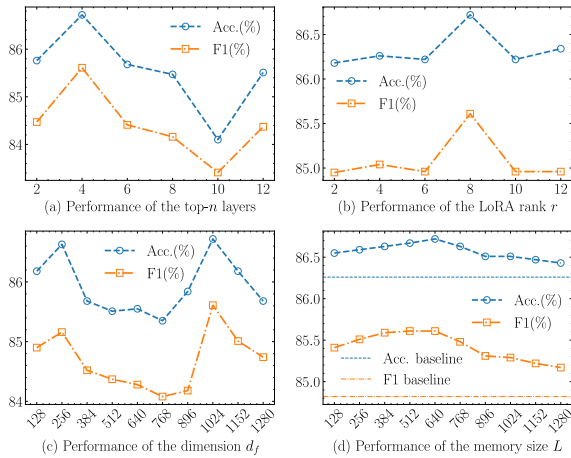


Figure 4: Hyperparameter study curves for InterCLIP-MEP w/ T2V. Panel (d) compares results with those from using only the classification module  $\mathcal{F}_c$  for prediction.

w/o Inter, the w/o MEP variant performed worse than the w/o Proj variant. However, for methods InterCLIP-MEP w/ T2V and InterCLIP-MEP w/ V2T, the w/o MEP variant performs better than the w/o Proj variant. This suggests that backbones with strong image-text interaction capabilities benefit from training the classification module  $\mathcal{F}_c$  along with the projection module  $\mathcal{F}_p$ , even without using MEP during inference. We also find that not using LoRA to fine-tune the self-attention modules results in significant performance loss, indicating that the original CLIP’s vanilla space is not directly suitable for the sarcasm detection task.

## Hyperparameter Study

In this section, we further investigate the method using Interactive-CLIP with T2V interaction as the backbone. Keeping the other hyperparameters constant, we condition different top- $n$  layers of the self-attention modules. We also study the impact of different projection dimensions  $d_f$ , different LoRA ranks  $r$ , and different memory sizes  $L$  on the InterCLIP-MEP w/ T2V method. We present all results in Figure 4. Figure 4(a) shows that conditioning the top four self-attention layers yields the best results. From Figure 4(b), a rank of 8 is optimal. Figure 4(c) indicates the projection dimension is best at 256 or 1024. Figure 4(d) reveals that a memory size of 640 in MEP outperforms others, confirming the value of historical sample knowledge.

## Case Study and Visualization

As shown in Figure 5, we select three examples to further demonstrate the robustness of InterCLIP-MEP. We observe that direct predictions through the classification module  $\mathcal{F}_c$  result in high prediction entropy and incorrect outcomes. However, MEP effectively mitigates the issue for cases where  $\mathcal{F}_c$  fails to correctly identify the results by using the historical knowledge of the test samples. To further validate that InterCLIP can more effectively capture the interactive information between text and images compared to orig-



Sample	Prediction
 <p>i'm pretty sure this cookie cake isn't big enough.</p>	GT: 😊 MEP: 😊 ✓ $\mathcal{F}_c$ : 😞 (entropy=0.58) ✗
<p>Teacher: You can't write an essay overnight. Exam: You have one hour to write an essay.</p> <p>everything is a test</p>	GT: 😊 MEP: 😊 ✓ $\mathcal{F}_c$ : 😞 (entropy=0.60) ✗
 <p>the trees are so beautiful i shed a tear</p>	GT: 😊 MEP: 😊 ✓ $\mathcal{F}_c$ : 😞 (entropy=0.66) ✗

Figure 5: Case study of InterCLIP-MEP.


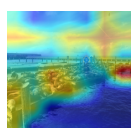
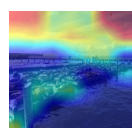
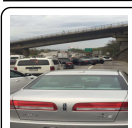
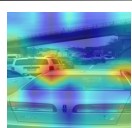
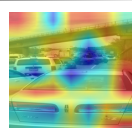
Sample	InterCLIP	CLIP
 <p>it smells wonderful out here !! – at sea lions at pier &lt;num&gt;</p>		
 <p>pinch me i'm dreaming ! atlanta traffic at its best folks</p>		

Figure 6: Visual comparison between InterCLIP and CLIP.

inal CLIP, thereby aiding in the detection of sarcasm cues, we visualize the areas of focus during the inference process of the visual model in Figure 6. We observe that in the first example, which complains about the unpleasant odor caused by the sea lions, InterCLIP focuses more accurately on the location of the sea lions compared to the original CLIP. In the second example, which complains about traffic congestion, InterCLIP correctly focuses on the distribution of cars on the road, whereas the original CLIP’s focus is scattered.

## Conclusion

In this paper, we propose a novel framework for robust multi-modal sarcasm detection, termed InterCLIP-MEP. We introduce an Interactive CLIP (InterCLIP) as the backbone for extracting sample representations. Unlike the original CLIP, InterCLIP embeds representations from different modalities into the encoder, effectively capturing the intricate interactions between text and image. For inference, we introduce a Memory-Enhanced Predictor (MEP) that leverages historical knowledge of valuable test samples to enhance inference, providing a more robust and reliable multi-modal sarcasm detection. Our experimental results demonstrate that InterCLIP-MEP achieves state-of-the-art performance on the MMSD2.0 benchmark.

## References

- Amir, S.; Wallace, B. C.; Lyu, H.; Carvalho, P.; and Silva, M. J. 2016. Modelling Context with User Embeddings for Sarcasm Detection in Social Media. In Riezler, S.; and Goldberg, Y., eds., *Proceedings of the 20th SIGNLL Conference on Computational Natural Language Learning*, 167–177. Berlin, Germany: Association for Computational Linguistics.
- Baddeley, A. D. 2000. The episodic buffer: a new component of working memory? *Trends in Cognitive Sciences*, 4: 417–423.
- Baziotis, C.; Nikolaos, A.; Papalampidi, P.; Kolovou, A.; Paraskevopoulos, G.; Ellinas, N.; and Potamianos, A. 2018. NTUA-SLP at SemEval-2018 Task 3: Tracking Ironic Tweets using Ensembles of Word and Character Level Attentive RNNs. In Apidianaki, M.; Mohammad, S. M.; May, J.; Shutova, E.; Bethard, S.; and Carpuat, M., eds., *Proceedings of the 12th International Workshop on Semantic Evaluation*, 613–621. New Orleans, Louisiana: Association for Computational Linguistics.
- Bouazizi, M.; and Ohtsuki, T. 2015. Sarcasm detection in twitter:” all your products are incredibly amazing!!!”-are they really? In *2015 IEEE global communications conference (GLOBECOM)*, 1–6. IEEE.
- Cai, Y.; Cai, H.; and Wan, X. 2019. Multi-Modal Sarcasm Detection in Twitter with Hierarchical Fusion Model. In *Annual Meeting of the Association for Computational Linguistics*.
- Devlin, J.; Chang, M.-W.; Lee, K.; and Toutanova, K. 2019. BERT: Pre-training of Deep Bidirectional Transformers for Language Understanding. *North American Chapter of the Association for Computational Linguistics*.
- Dosovitskiy, A.; Beyer, L.; Kolesnikov, A.; Weissenborn, D.; Zhai, X.; Unterthiner, T.; Dehghani, M.; Minderer, M.; Heigold, G.; Gelly, S.; Uszkoreit, J.; and Houshy, N. 2021. An Image is Worth 16x16 Words: Transformers for Image Recognition at Scale. In *International Conference on Learning Representations*.
- Ganz, R.; Kittenplon, Y.; Aberdam, A.; Ben Avraham, E.; Nuriel, O.; Mazor, S.; and Litman, R. 2024. Question Aware Vision Transformer for Multimodal Reasoning. In *Proceedings of the IEEE/CVF Conference on Computer Vision and Pattern Recognition (CVPR)*, 13861–13871.
- Gibbs, R.; and Colston, H. 2007. *Irony in Language and Thought: A Cognitive Science Reader*. Lawrence Erlbaum Associates. ISBN 9780805860627.
- Gibbs, R. W.; and O’Brien, J. 1991. Psychological aspects of irony understanding. *Journal of Pragmatics*, 16(6): 523–530.
- Graves, A.; and Schmidhuber, J. 2005. Framewise phoneme classification with bidirectional LSTM and other neural network architectures. *Neural Networks*, 18(5): 602–610. IJCNN 2005.
- He, K.; Zhang, X.; Ren, S.; and Sun, J. 2016. Deep Residual Learning for Image Recognition. In *2016 IEEE Conference on Computer Vision and Pattern Recognition (CVPR)*, 770–778.
- Hu, E. J.; Shen, Y.; Wallis, P.; Allen-Zhu, Z.; Li, Y.; Wang, S.; Wang, L.; and Chen, W. 2022. LoRA: Low-Rank Adaptation of Large Language Models. In *International Conference on Learning Representations*.
- Kim, Y. 2014. Convolutional Neural Networks for Sentence Classification. In Moschitti, A.; Pang, B.; and Daelemans, W., eds., *Proceedings of the 2014 Conference on Empirical Methods in Natural Language Processing (EMNLP)*, 1746–1751. Doha, Qatar: Association for Computational Linguistics.
- Li, J.; Shakhnarovich, G.; and Yeh, R. A. 2022. Adapting CLIP For Phrase Localization Without Further Training. *arXiv preprint arXiv: 2204.03647*.
- Liang, B.; Lou, C.; Li, X.; Gui, L.; Yang, M.; and Xu, R. 2021. Multi-modal sarcasm detection with interactive in-modal and cross-modal graphs. In *Proceedings of the 29th ACM international conference on multimedia*, 4707–4715.
- Liang, B.; Lou, C.; Li, X.; Yang, M.; Gui, L.; He, Y.; Pei, W.; and Xu, R. 2022. Multi-Modal Sarcasm Detection via Cross-Modal Graph Convolutional Network. In *Annual Meeting of the Association for Computational Linguistics*.
- Liang, F.; Wu, B.; Dai, X.; Li, K.; Zhao, Y.; Zhang, H.; Zhang, P.; Vajda, P.; and Marculescu, D. 2023. Open-Vocabulary Semantic Segmentation With Mask-Adapted CLIP. In *Proceedings of the IEEE/CVF Conference on Computer Vision and Pattern Recognition (CVPR)*, 7061–7070.
- Liu, H.; Wang, W.; and Li, H. 2022. Towards Multi-Modal Sarcasm Detection via Hierarchical Congruity Modeling with Knowledge Enhancement. In *Conference on Empirical Methods in Natural Language Processing*.
- Liu, Y.; Ott, M.; Goyal, N.; Du, J.; Joshi, M.; Chen, D.; Levy, O.; Lewis, M.; Zettlemoyer, L.; and Stoyanov, V. 2019. RoBERTa: A Robustly Optimized BERT Pretraining Approach. *arXiv preprint arXiv: 1907.11692*.
- Muecke, D. C. 1982. *Irony and the Ironic*. New York: Methuen.
- Pan, H.; Lin, Z.; Fu, P.; Qi, Y.; and Wang, W. 2020. Modeling Intra and Inter-modality Incongruity for Multi-Modal Sarcasm Detection. In Cohn, T.; He, Y.; and Liu, Y., eds., *Findings of the Association for Computational Linguistics: EMNLP 2020*, 1383–1392. Online: Association for Computational Linguistics.
- Pang, B.; Lee, L.; et al. 2008. Opinion mining and sentiment analysis. *Foundations and Trends® in information retrieval*, 2(1–2): 1–135.
- Qin, L.; Huang, S.; Chen, Q.; Cai, C.; Zhang, Y.; Liang, B.; Che, W.; and Xu, R. 2023. MMSD2.0: Towards a Reliable Multi-modal Sarcasm Detection System. In Rogers, A.; Boyd-Graber, J.; and Okazaki, N., eds., *Findings of the Association for Computational Linguistics: ACL 2023*, 10834–10845. Toronto, Canada: Association for Computational Linguistics.
- Radford, A.; Kim, J. W.; Hallacy, C.; Ramesh, A.; Goh, G.; Agarwal, S.; Sastry, G.; Askell, A.; Mishkin, P.; Clark, J.; et al. 2021. Learning transferable visual models from natural language supervision. In *International conference on machine learning*, 8748–8763. PMLR.



- Schifanella, R.; De Juan, P.; Tetreault, J.; and Cao, L. 2016. Detecting sarcasm in multimodal social platforms. In *Proceedings of the 24th ACM international conference on Multimedia*, 1136–1145.
- Stokes, M. G. 2015. ‘Activity-silent’ working memory in prefrontal cortex: a dynamic coding framework. *Trends in cognitive sciences*, 19(7): 394–405.
- Sukhbaatar, S.; Weston, J.; Fergus, R.; et al. 2015. End-to-end memory networks. *Advances in neural information processing systems*, 28.
- Tian, Y.; Xu, N.; Zhang, R.; and Mao, W. 2023. Dynamic Routing Transformer Network for Multimodal Sarcasm Detection. In *Annual Meeting of the Association for Computational Linguistics*.
- Tsur, O.; Davidov, D.; and Rappoport, A. 2010. ICWSM — A Great Catchy Name: Semi-Supervised Recognition of Sarcastic Sentences in Online Product Reviews. *Proceedings of the International AAAI Conference on Web and Social Media*, 4(1): 162–169.
- Wang, Q.; Du, J.; Yan, K.; and Ding, S. 2023. Seeing in Flowing: Adapting CLIP for Action Recognition with Motion Prompts Learning. In *Proceedings of the 31st ACM International Conference on Multimedia*, 5339–5347.
- Wei, Y.; Yuan, S.; Zhou, H.; Wang, L.; Yan, Z.; Yang, R.; and Chen, M. 2024. G2SAM: Graph-Based Global Semantic Awareness Method for Multimodal Sarcasm Detection. *Proceedings of the AAAI Conference on Artificial Intelligence*, 38(8): 9151–9159.
- Wen, C.; Jia, G.; and Yang, J. 2023. Dip: Dual incongruity perceiving network for sarcasm detection. In *Proceedings of the IEEE/CVF Conference on Computer Vision and Pattern Recognition*, 2540–2550.
- Weston, J.; Chopra, S.; and Bordes, A. 2014. Memory Networks. *International Conference on Learning Representations*.
- Wu, Z.; Xiong, Y.; Yu, S. X.; and Lin, D. 2018. Unsupervised feature learning via non-parametric instance discrimination. In *Proceedings of the IEEE conference on computer vision and pattern recognition*, 3733–3742.
- Xiong, T.; Zhang, P.; Zhu, H.; and Yang, Y. 2019. Sarcasm Detection with Self-matching Networks and Low-rank Bilinear Pooling. In *The World Wide Web Conference, WWW ’19*, 2115–2124. New York, NY, USA: Association for Computing Machinery. ISBN 9781450366748.
- Xu, N.; Zeng, Z.; and Mao, W. 2020. Reasoning with multimodal sarcastic tweets via modeling cross-modality contrast and semantic association. In *Proceedings of the 58th annual meeting of the association for computational linguistics*, 3777–3786.
- Zhang, Y.; Zhu, W.; Tang, H.; Ma, Z.; Zhou, K.; and Zhang, L. 2024. Dual Memory Networks: A Versatile Adaptation Approach for Vision-Language Models. In *Proceedings of the IEEE/CVF conference on computer vision and pattern recognition*.